J|A|C|S
ARTICLES

Published on Web 04/17/2009

Highly Efficient and Rapid Cs^+ Uptake by the Layered Metal Sulfide $K_{2x}Mn_xSn_{3-x}S_6$ (KMS-1)

Manolis J. Manos and Mercouri G. Kanatzidis*

Department of Chemistry, Northwestern University, 2145 Sheridan Road, Evanston, IL 6020-3113

Received February 14, 2009; E-mail: m-kanatzidis@northwestern.edu

Abstract: The details of the ion-exchange properties of the layered sulfide material $K_{2x}Mn_xSn_{3-x}S_6$ ($x = 0.5-0.95$) (KMS-1) with Cs^+ and Rb^+ cations are reported. X-ray photoelectron spectroscopy (XPS), elemental analyses, and powder and single-crystal diffraction studies revealed that the Cs^+ and Rb^+ ion exchange of KMS-1 is complete (quantitative replacement of K^+ ions) and topotactic. These data also revealed that the Cs^+ exchange is accompanied with a rare topotactic oxidation of Mn^{2+} to Mn^{3+} caused by atmospheric oxygen, while the Rb^+ ion exchange only slightly alters the oxidation state of the layer manganese atoms. The absorption of Cs^+ by KMS-1 follows the Langmuir model with a high exchange capacity of 226(4) mg/g (pH $\approx$ 7) and distribution coefficients as high as 2×10^4 mL/g. KMS-1 displays significant cesium uptake both under strongly acidic (pH 0.7−2.6) or basic conditions (pH 10−12). The kinetics of Cs^+ capture by KMS-1 is fast (>90% removal of ~1 ppm of Cs^+ within only 5 min). KMS-1 was also found capable to efficiently absorb Cs^+ from complex solutions containing various competitive cations in large excess. KMS-1 (containing Mn^{3+} ions) can be regenerated and reused for Cs^+ exchange with an exchange capacity very similar to that of the pristine KMS-1. The results indicate that layered metal sulfides with ion-exchange properties may be considered as highly selective and cost-effective sorbents for remediation of water contaminated with the radioactive ^{137}Cs isotope. The selectivity over other alkali ions for Cs originates not from a size effect but from the more favorable Cs···S soft Lewis acid/Lewis base interactions.

Introduction

The variety of layered compounds known is astonishing. These include clays, layered double hydroxides (LDHs), transition metal oxides, metal oxo- or thiophosphates, oxy-halides, and oxy-sulfides.[1−] A great deal of attention has been paid to the clays and LDHs because of their natural abundance and useful properties.[1–19] Specifically, the clays composed of aluminosilicate anionic slabs and alkali or alkaline earth counter cations are excellent cationic exchangers capable of incorporating a variety of guest ions ranging from simple inorganic ions to bulky organic species (e.g.[26], fullerenes[11,12]).[1–13] Their ion-exchange properties have found applications in diverse fields

(1) Swartzen-Allen, S. L.; Matijevic, E. *Chem. Rev.* **1974**, *74*, 385–400.
(2) Suib, S. L. *Chem. Rev.* **1993**, *93*, 803–26.
(3) Ogawa, M.; Kuroda, K. *Chem. Rev.* **1995**, *95*, 399–438.
(4) (a) Dumat, C.; Quiquampoix, H.; Staunton, S. *Environ. Sci. Technol.* **2000**, *34*, 2985–2989. (b) Kanatzidis, M. G.; Marcy, H.; McCarthy, W. J.; Kannewurf, C. R.; Marks, T. J. *Solid State Ionics* **1989**, 594–608. (c) Wang, L.; Brazis, P.; Rocci, M.; Kannewurf, C. R.; Kanatzidis, M. G. *Chem. Mater.* **1998**, *10*, 3298–3300.
(5) Celis, R.; HermosIn, M. C.; Cornejo, J. *Environ. Sci. Technol.* **2000**, *34*, 4593–4599.
(6) Ijdo, W. L.; Pinnavaia, T. J. *Green Chem.* **2001**, *3*, 10–12.
(7) (a) Pinnavaia, T. J. *Science* **1983**, *220*, 365–71. (b) Liu, Y. J.; DeGroot, D. C.; Schindler, J. L.; Kannewurf, C. R.; Kanatzidis, M. G. *J. Chem. Soc. Chem. Commun.* **1993**, 593–596. (c) Wang, L.; Rocci-Lane, M.; Brazis, P.; Kannewurf, C. R.; Kim, Y.-I.; Lee, W.; Choy, J.-H.; Kanatzidis, M. G. *J. Am. Chem. Soc.* **2000**, *122*, 6629–6640.
(8) Ijdo, W. L.; Lee, T.; Pinnavaia, T. J. *Adv. Mater.* **1996**, *8*, 79–83.
(9) Triantafillidis, C. S.; LeBaron, P. C.; Pinnavaia, T. J. *Chem. Mater.* **2002**, *14*, 4088–4095.
(10) Thomas, S.; Bertrand, J. A.; Occelli, M. L. *Chem. Mater.* **1999**, *11*, 184–187.
(11) Gournis, D.; Georgakilas, V.; Karakassides, M. A.; Bakas, T.; Kordatos, K.; Prato, M.; Fanti, M.; Zerbetto, F. *J. Am. Chem. Soc.* **2004**, *126*, 8561–8568.
(12) Gournis, D.; Jankovic, L.; Maccallini, E.; Benne, D.; Rudolf, P.; Colomer, J.-F.; Sooambar, C.; Georgakilas, V.; Prato, M.; Fanti, M.; Zerbetto, F.; Sarova, G. H.; Guldi, D. M. *J. Am. Chem. Soc.* **2006**, *128*, 6154–6163.
(13) Pless, J. D.; Maxwell, R. S.; Philips, M. L. F.; Helean, K. B.; Axness, M. Y.; Nenoff, T. M. *Chem. Mater.* **2005**, *17*, 5101–5108.
(14) Williams, G. R.; O'Hare, D. *J. Mater. Chem.* **2006**, *16*, 3065–3074.
(15) Liu, Z.; Ma, R.; Osada, M.; Iyi, N.; Ebina, Y.; Takada, K.; Sasaki, T. *J. Am. Chem. Soc.* **2006**, *128*, 4872–4880.
(16) Choudary, B. M.; Madhi, S.; Chowdari, N. S.; Kantam, M. L.; Sreedhar, B. *J. Am. Chem. Soc.* **2002**, *124*, 14127–14136.
(17) Roeffaers, M. B. J.; Sels, B. F.; Uji-i, H.; De Schryver, F. C.; Jacobs, P. A.; De Vos, D. E.; Hofkens, J. *Nature (London)* **2006**, *439*, 572–575.
(18) Sels, B.; De Vos, D.; Buntinx, M.; Pierard, F.; Kirsch-De Mesmaeker, A.; Jacobs, P. *Nature (London)* **1999**, *400*, 855–857.
(19) Fujita, W.; Awaga, K. *Inorg. Chem.* **1996**, *35*, 1915–17.
(20) Ma, Y.; Suib, S. L.; Ressler, T.; Wong, J.; Lovallo, M.; Tsapatsis, M. *Chem. Mater.* **1999**, *11*, 3545–3554.
(21) Olivera-Pastor, P.; Maireles-Torres, P.; Rodriguez-Castellon, E.; Jimenez-Lopez, A.; Cassagneau, T.; Jones, D. J.; Roziere, J. *Chem. Mater.* **1996**, *8*, 1758–1769.
(22) Lacroix, P. G.; Clement, R.; Nakatani, K.; Zyss, J.; Ledoux, I. *Science* **1994**, *263*, 658–60.
(23) Clement, R.; Lacroix, P. G.; O'Hare, D.; Evans, J. *Adv. Mater.* **1994**, *6*, 794–7.
(24) Benard, S.; Leaustic, A.; Riviere, E.; Yu, P.; Clement, R. *Chem. Mater.* **2001**, *13*, 3709–3716.
(25) Indris, S.; Cabana, J.; Rutt, O. J.; Clarke, S. J.; Grey, C. P. *J. Am. Chem. Soc.* **2006**, *128*, 13354–13355.

including environmental remediation, catalysis and nanocomposites.[4–9] LDHs, also known as anionic clays, are expressed by the general formula $[M^{II}_{1-x}M^{III}_{x}(OH)_2][A^{n-}_{x/n}\cdot mH_2O]$ and represent rare examples of anionic exchangers useful as adsorbents, neutralizers, catalysts, optical, and magnetic materials.[3,14–19]

The ion-exchange chemistry of layered metal chalcogenides is relatively little explored compared to that of oxidic ion exchangers. Actually, layered chalcogenides with ion-exchange properties are relatively few. These are mainly limited to alkali ion-containing transition metal dichalcogenides A_xMQ_2 (A = alkali ion; M = early transition metal from groups 4, 5, and 6, Q = S, Se, Te).[27−37] The hydrolytic instability of such materials, however, prohibits their use in extensive ion-exchange investigations.[27–37]

KMS-1 is a layered sulfide of the formula $K_{2x}Mn_xSn_{3-x}S_6$ (x = 0.5−0.95), recently reported by our group. This low-cost material consisting of relatively nontoxic elements was proved excellent sorbent for Sr^{2+}, particularly under extremely alkaline conditions (pH ≥ 13) and with large excess of Na^+.[38] This property of the material is particularly interesting for remediation of nuclear wastes.[39,40] In addition, KMS-1 showed an extraordinarily high selectivity to absorb soft heavy metal ions (Hg^{2+}, Pb^{2+}, Cd^{2+}) arising from the strong covalent interactions of these metal ions with the sulfide framework of KMS-1.[41]

The high stability of KMS-1 under ambient conditions and in water solutions of wide pH range makes it an ideal system for fundamental ion-exchange studies. Such studies help us to gain insight into the largely unknown ion-exchange chemistry of chalcogenides and design new chalcogenide materials with improved ion-exchange properties.

Herein, we report the ion-exchange properties of KMS-1 with Cs^+ and Rb^+ ions. Employing a variety of spectroscopic and analytical techniques including X-ray single-crystal diffraction, we show not only that the exchange of the K^+ ions of KMS-1 by Cs^+ and Rb^+ is complete and topotactic but also that it results (in the case of Cs^+) in an unusual topotactic oxidation of Mn^{2+} to Mn^{3+} with formation of rare examples of stable Mn^{3+}-containing sulfides. Through detailed investigations in aqueous solutions of various compositions and pH values, we also demonstrate the high efficiency of KMS-1 as a selective sorbent for Cs^+ ions, the radioactive version of which represents one of the major contaminants in the fission product of nuclear wastes.[39,40]

Experimental Section

Materials. Sn was purchased from Aldrich Chemical Co, 325 mesh, 99.8%. Mn was purchased from Cerac Inc., −325 mesh, >99.5%. Sublimed sulfur was purchased from J. T. Baker Chemical Co., >99.5%. CsCl, RbI, and KCl were purchased from Aldrich Chemical Co. The preparation of Cs_2S is described in ref 42.

Synthesis of $K_{2x}Mn_xSn_{3-x}S_6$ (1) (x = 0.5−0.95) (KMS-1). The syntheses of these materials are described in ref 38.

Cs^+ and Rb^+ Ion Exchange with Single Crystals of $K_{1.90}Mn_{0.95}Sn_{2.05}S_6$. Single crystals of $K_{1.9}Mn_{0.95}Sn_{2.05}S_6$ (10 mg, 0.018 mmol) were placed in an aqueous solution (10 mL) of CsCl or RbI (0.24 mmol). The mixture was then heated at 70 °C and left undisturbed at this temperature for 1 week. The crystals were then isolated with filtration and washed several times with water, acetone, and diethyl ether. EDS on several of them revealed the average formula "$Cs_{0.9}MnSn_{2.5}S_{5.5}$" or "$Rb_{1.7}MnSn_{2.4}S_{5.5}$". According to single-crystal X-ray analysis, the exchanged crystals correspond to the compound $CsMn_{0.95}Sn_{2.05}S_6$ or $Rb_{1.57}Mn_{0.95}Sn_{2.05}S_6$.

Solid-State Synthesis of $Cs_{2x}Mn_xSn_{3-x}S_6$ (x = 0.5−0.95). This compound was synthesized for comparison purposes with the Cs-exchanged KMS-1 material. A mixture of Sn (1.9 mmol, 226 mg), Mn (1.1 mmol, 60 mg), Cs_2S (2 mmol, 596 mg), and S (16 mmol, 512 mg) was sealed under vacuum (10^{-4} Torr) in a silica tube and heated (50 °C/h) to 500 (or 400) °C for 60 h, followed by cooling to room temperature at 50 °C/h. The excess flux was removed with H_2O or dimethylformamide (DMF, Aldrich) to reveal dark brown polycrystalline material $Cs_{2x}Mn_xSn_{3-x}S_6$ (x = 0.5−0.95) and orange crystals as a minor phase. The dark brown polycrystalline materials were manually separated by orange crystals which coexisted in the product. The yield for the preparation of $Cs_{2x}Mn_xSn_{3-x}S_6$ (x = 0.5−0.95) was 70−80%. The orange crystals correspond to a quaternary phase with similar composition (found by EDS) as the dark brown phase but different structure based on PXRD. Efforts to solve the structure of this new material are underway.

Ion-Exchange Studies with Polycrystalline KMS-1. A typical ion-exchange experiment of KMS-1 with A^+ ions (A = Rb^+, Cs^+) is as follows. In a solution of ACl (1.0 mmol) in water, compound KMS-1 (0.07 mmol, 40 mg) was added as a solid. The mixture was kept under magnetic stirring or constant shaking for ∼12 h. Then, the dark brown polycrystalline material was isolated by filtration, washed several times with water, acetone, and ether, and dried in air. In all cases, the ion-exchange was completed after only one cycle.

The distribution coefficient K_d, used for the determination of the affinity and selectivity of compounds KMS-1 for Cs^+ is given by the equation $K_d = (V[(C_0 - C_f)/C_f])/(m)$ where C_0 and C_f are the initial and equilibrium concentration of M^{n+} (ppm), V is the volume (mL) of the testing solution, and m is the amount of the ion exchanger (g) used in the experiment.[38]

The Cs^+ uptake from solutions of various concentrations were studied by the batch method at $V/m \approx 1000$ mL/g, at room temperature and 12 h contact. The data obtained were used for the determination of Cs^+ sorption isotherms.

Competitive ion-exchange experiments of KMS-1 were also carried out with the batch method at V/m ratio 50−1000 mL/g, at room temperature and 12 h contact time.

For the regeneration of KMS-1, samples of ∼10 mg of Cs-laden KMS-1 were treated for ∼24 h with ∼10 mL water solutions containing 1 M KCl. No Cs^+ was detected in the regenerated

(26) Gal, Z. A.; Rutt, O. J.; Smura, C. F.; Overton, T. P.; Barrier, N.; Clarke, S. J.; Hadermann, J. *J. Am. Chem. Soc.* **2006**, *128*, 8530–8540.
(27) Heising, J.; Kanatzidis, M. G. *J. Am. Chem. Soc.* **1999**, *121*, 11720–11732.
(28) Petkov, V.; Billinge, S. J. L.; Heising, J.; Kanatzidis, M. G. *J. Am. Chem. Soc.* **2000**, *122*, 11571–11576.
(29) Bissessur, R.; Heising, J.; Hirpo, W.; Kanatzidis, M. *Chem. Mater.* **1996**, *8*, 318–20.
(30) Kanatzidis, M. G.; Bissessur, R.; DeGroot, D. C.; Schindler, J. L.; Kannewurf, C. R. *Chem. Mater.* **1993**, *5*, 595–6.
(31) Hwang, S.-J.; Petkov, V.; Rangan, K. K.; Shastri, S.; Kanatzidis, M. G. *J. Phys. Chem. B* **2002**, *106*, 12453–12458.
(32) Divigalpitiya, W. M. R.; Frindt, R. F.; Morrison, S. R. *Science* **1989**, *246*, 369–71.
(33) Dungey, K. E.; Curtis, M. D.; Penner-Hahn, J. E. *Chem. Mater.* **1998**, *10*, 2152–2161.
(34) Zak, A.; Feldman, Y.; Lyakhovitskaya, V.; Leitus, G.; Popovitz-Biro, R.; Wachtel, E.; Cohen, H.; Reich, S.; Tenne, R. *J. Am. Chem. Soc.* **2002**, *124*, 4747–4758.
(35) Whittingham, M. S. *Chem. Rev.* **2004**, *104*, 4271–4301.
(36) Morosan, E.; Zandbergen, H. W.; Dennis, B. S.; Bos, J. W. G.; Onose, Y.; Klimczuk, T.; Ramirez, A. P.; Ong, N. P.; Cava, R. J. *Nat. Phys.* **2006**, *2*, 544–550.
(37) Gash, A. E.; Spain, A. L.; Dysleski, L. M.; Flaschenriem, C. J.; Kalaveshi, A.; Dorhout, P. K.; Strauss, S. H. *Environ. Sci. Technol.* **1998**, *32*, 1007–1012.
(38) Manos, M. J.; Ding, N.; Kanatzidis, M. G. *Proc. Natl. Acad. Sci. U.S.A.* **2008**, *105*, 3696–3699.
(39) Mumpton, F. A. *Proc. Natl. Acad. Sci. U.S.A.* **1999**, *96*, 3463–3470.
(40) Seever, W. J. *Handbook of Complex Environmental Remediation Problems*; McGraw-Hill Professional: Blacklick, OH, 2001.
(41) Manos, M. J.; Kanatzidis, M. G. Chem.—Eur. J. (in press).
(42) Liao, J. H.; Varotsis, C.; Kanatzidis, M. G. *Inorg. Chem.* **1993**, *32*, 2453–62.

Table 1. Selected Crystallographic Data for Compounds KMS-1 (from Ref 38) and the Cs- and Rb-Exchanged Compounds

formula	$K_{1.90(3)}Mn_{0.95(1)}Sn_{2.05(2)}S_6$	$Cs_{1.00(4)}Mn_{0.95(1)}Sn_{2.05(4)}S_6$	$Rb_{1.57(3)}Mn_{0.95(2)}Sn_{2.05(3)}S_6$
formula weight	562.16	620.78	622.06
temperature, K	293(2)	293(2)	293(2)
space group	$R\bar{3}m$	$R\bar{3}m$	$R\bar{3}m$
a, Å	3.6969(5)	3.6139(8)	3.6827(4)
c, Å	25.403(5)	26.867(12)	25.934(6)
V, Å^3, Z	300.67(8), 1	303.88(17), 1	304.60(8), 1
d_{calc}, g/cm^3	3.105	3.392	3.391
μ, mm^{-1}	6.845	9.072	12.338
$2\theta_{max}$, deg	53.52	53.40	53.80
reflections collected	989	1057	637
unique reflections (total)	110 ($R_{int} = 0.0482$)	112 ($R_{int} = 0.1190$)	113 ($R_{int} = 0.054$)
unique reflections [$I > 2\sigma(I)$]	108	105	109
no. of variables	12	12	13
GOF on F^2	1.192	1.188	1.260
final R1[a]/wR2,[b] %	2.64/6.58	6.50/16.99	4.06/9.86
largest diff. peak/hole (e•A^{-3})	1.519/−0.995	2.547/−1.168	2.055/−1.407

[a] $R1 = \sum ||F_o| - |F_c||/\sum|F_o|$. [b] $wR2 = \{\sum [w(F_o^2 - F_c^2)^2]/\sum[w(F_o^2)^2]\}^{1/2}$.

samples with ICP-MS, while the ratio K/Mn found by ICP-AES for these samples was ∼1. To test the reusability of the regenerated samples, samples of ∼10 mg were treated with 10 mL solutions containing ∼550 ppm of Cs^+. The Cs^+ content of the solutions after these ion exchange reactions was determined by ICP-MS.

The kinetic studies of Cs^+ absorption by KMS-1 were carried out as follows. Ion-exchange experiments of various reaction times (5, 10, 15, 30, 40, 60, 120, and 1200 min) were performed. For each experiment, a total of 10 mg of compound KMS-1 was weighted into a 20 mL glass vial. A 10 mL sample of water solution containing ∼1 ppm of Cs^+ was added to each vial, and the mixtures were kept under magnetic stirring for the designated reaction times. The suspensions from the various reactions were filtered (through filter paper, Whatman No. 1), and the filtrates were analyzed for their Cs^+ content with inductively coupled plasma-mass spectroscopy (ICP-MS).

Powder X-ray Diffraction (PXRD). The samples were examined by PXRD for identification purposes and to assess phase purity. Powder patterns were obtained using a CPS 120 INEL X-ray powder diffractometer with Ni-filtered Cu Kα radiation operating at 40 kV and 20 mA and equipped with a position-sensitive detector. Samples were ground and spread on a glass slide. The purity of phases was confirmed by comparison of the X-ray powder diffraction patterns to ones calculated from single-crystal data using the NIST Visualize 1.0.1.2 software.

EDS Analyses. The analyses were performed using a JEOL JSM-6400V scanning electron microscope (SEM) equipped with a Tracor Northern energy dispersive spectroscopy (EDS) detector. Data acquisition was performed with an accelerating voltage of 25 kV and 40 s accumulation time.

XPS (X-ray Photoelectron Spectroscopy) Analysis. XPS was performed on a Perkin-Elmer Phi 5400 ESCA system equipped with a Mg Kα X-ray source. Samples were analyzed at pressures between 10^{-9} and 10^{-8} torr with a pass energy of 29.35 eV and a takeoff angle of 45°. All peaks were referred to the signature C1s peak for adventitious carbon at 284.6 eV. Fitting of the peaks has been made by using the software XPSPEAK41.

Thermal Analysis. Thermogravimetric analysis (TGA) was carried out with a Shimatzu TGA 50. Samples (10 ± 0.5 mg) were placed in quartz crucible. Samples were heated from ambient temperature to 500 °C in a 20 mL/min flow of N_2 or air. Heating rate of 10 °C/min was used and continuous records of sample temperature, sample weight and its first derivative (DTG) were taken.

Inductively Coupled Plasma-Atomic Emission (Optical Emission)/ [ICP-AES(OES)] Analyses. The content of Na^+, Ca^{2+}, Mg^{2+}, and K^+ of the complex water solutions was also determined by ICP-AES using VISTA MPX CCD SIMULTANEOUS ICP-OES instrument. Standards of the ions of interest (K^+, Ca^{2+}, Mg^{2+}, and Na^+) were prepared by diluted commercial (Aldrich or GFS chemicals) ∼1000 ppm ICP standards of these ions. The calibration was linear or quadratic with maximum errors of 5−10%. The ICP-AES intensity was the result of three (30 s) exposures. For each sample, three readings of the ICP-AES intensity were recorded and averaged.

ICP-MS Analyses. Cs^+ displays weak emission and can be analyzed only with ICP-MS. To determine the amount of Cs, a computer-controlled Thermo Elemental (Waltham, MA) PQ ExCell inductively coupled plasma mass spectrometer (ICP-MS) with a quadruple setup was used. Quadrupole ICP-MS is capable of identifying elements from ppt-ppb levels. Ten standards of Cs^+ in the range of 1−40 ppb were prepared by diluting a commercial (Aldrich) ∼1000 ppm Cs^+ solution. The samples were diluted to lower the concentrations below than 40 ppb. All samples (including standards) were prepared in a 3% nitric acid solution with 2 ppb ^{153}Eu internal standard in order to correct for instrumental drift and matrix effects during analysis. The ^{133}Cs isotope was analyzed.

Single-Crystal X-ray Crystallography. A Siemens SMART Platform CCD diffractometer operating at room temperature and using graphite-monochromatized Mo Kα radiation, was used for data collection. The data were collected at 293(2) K over a full sphere of reciprocal space, up to 27−28° in θ. Cell refinement and data reduction were carried out with the program SAINT.[43] An empirical absorption correction was done to the data using SADABS.[43] The intensities were extracted by the program XPREP.[44] The structures were solved with direct methods using SHELXS and least-squares refinement were done against F_{obs}^2 using routines from SHELXTL software.[44] The K, Rb, and Cs atom positions in the structures of $K_{1.9}Mn_{0.95}Sn_{2.05}S_6$, $Rb_{1.57}Mn_{0.95}Sn_{2.05}S_6$, and $CsMn_{0.95}Sn_{2.05}S_6$ were modeled as split sites. Selected crystal data for the structures of compounds are given in Table 1. Further details of the crystal structure investigations may be obtained by the crystallographic information files (CIFs) (see Supporting Information).

Results and Discussion

Ion-Exchange of KMS-1 with Cs^+ and Rb^+ Ions. The disordered state of the K^+ ions in KMS-1 implies high ion mobility and good ion-exchange properties. Indeed, polycrystalline samples of KMS-1 can completely replace the K^+ ions with Cs^+ and Rb^+ after a few hours of ion exchange, even when using low concentrations of these ions. The complete replacement of K^+ ions was confirmed by EDS analysis.

(43) Siemens Analytical X-Ray Instruments Inc. 1995.
(44) Sheldrick, G. M. *SHELXTL, version 5.1*; Bruker-AXS: Madison, WI, 1998.

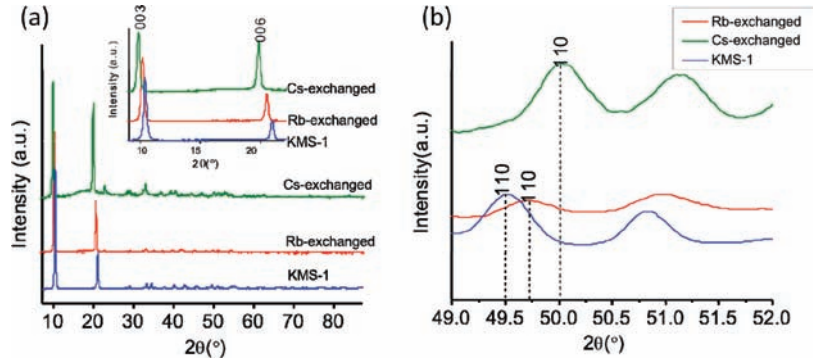

Figure 1. (a) PXRD patterns for the pristine KMS-1, Cs^+-, and Rb^+-exchanged materials. An enlarged view of the (003) and (006) reflection peaks is given in the inset. (b) The (110) reflection peaks for the pristine, Cs-, and Rb-exchanged compounds, showing the anomalous trend in the diffraction angle. The shift of (110) to higher 2θ angle in the Cs-exchanged material reflects the presence of Mn^{3+} in this system.

PXRD measurements showed that the exchanged materials are isostructural with the pristine confirming a topotactic ion exchange (Figure 1). A shift of the (003) and (006) Bragg peaks to lower 2θ values (or higher d-spacing) was observed in the diffraction patterns of Cs^+- and Rb^+-exchanged products (inset of Figure 1a). The c-axis lengths, estimated by the position of the (003) reflection [i.e., by multiplying $3d_{003}$], follow the order: Cs^+ (27.05 Å) > Rb^+ (26.12 Å) > pristine (25.59−25.98 Å). This order is consistent with the size of the intercalated cations. The hydration state of the materials was determined by TGA measurements (see Supporting Information). Namely, the degree of hydration increases with the order Cs-exchanged (1.8 H_2O) < Rb^+-exchanged (2.7 H_2O) ≈ pristine (2−3 H_2O).

Despite the strong preferred orientation due to the platelike shape of the materials, some (hk0) reflections were discernible in the PXRD patterns of pristine, Rb^+-, and Cs^+-exchanged products, which can be used to determine the a-axis lengths of these materials (Figure 1b). Specifically, for a structure with $R\bar{3}m$ space group the a axis can be obtained by doubling the d-spacing value for the (110) reflection. For the Rb^+-exchanged materials, the a axis was calculated to be 3.67 Å, very close to that of the pristine compound (3.68 Å). The Cs^+-exchanged materials, however, tended to possess a shorter a axis (∼3.64−3.65 vs 3.68−3.69 Å for the K analogue).

The Cs/Mn or Rb/Mn ratio in the exchanged materials should be equal to 2 to satisfy the charge-balance requirements. This means that the formula of the compounds should be analogous to starting material KMS-1, i.e., $Cs_{2x}Mn_xSn_{3-x}S_6$ or $Rb_{2x}Mn_xSn_{3-x}S_6$ ($x = 0.5-0.95$). However, EDS analysis gave lower Rb/Mn ratios in the range of 1.4−1.7. More surprisingly, the Cs^+-exchanged materials showed a Cs/Mn ratio of only ∼1:1. These low ratios were puzzling and could not be attributed to partial ion-exchange since the materials did not contain any potassium.

Single-Crystal Studies. To obtain more detailed insight into these unexpected results and precisely determine the actual structure/composition of the Cs^+- and Rb^+-exchanged products, we conducted ion-exchange experiments using single crystals of $K_{1.9}Mn_{0.95}Sn_{2.05}S_6$ and succeeded in obtaining diffraction-quality crystals for a detailed crystallographic analysis. The X-ray diffraction refinement (Table 1), essentially confirmed the results of EDS analysis and gave the formulas $CsMn_{0.95}Sn_{2.05}S_6$ and $Rb_{1.57}Mn_{0.95}Sn_{2.05}S_6$, respectively. According to these formulas, the average Mn oxidation state must be +3 and +2.3 in the Cs^+- and Rb^+-exchanged compounds, respectively.

The a-cell parameter found by the single-crystal diffraction data for the Cs^+ and Rb^+ analogues were 3.6139(8) and 3.6827(4) Å, respectively, which are significantly smaller than that (3.6969(5) Å) of the pristine material. The shrinkage of the a axis after ion-exchange (along with the shortening of the "Mn/Sn"−S bonds) reflects the oxidation of Mn^{2+} ions to the smaller Mn^{3+} ions. The stability of a higher Mn oxidation state in the Cs^+-exchanged product may be explained with the concept of Lewis acid/base. Cs^+ is less Lewis acidic than Rb^+ and K^+. Thus, the Lewis basicity of $[Mn_xSn_{3-x}S_6]^{2x-}$ when Cs^+ is the counterion is higher than when Rb^+ and K^+ are the counterions and this may facilitate the oxidation of manganese. In other words, Cs^+ ions make its conjugate base (in this case $[Mn_xSn_{3-x}S_6]^{2x-}$) more electron rich because it provides the most ionic (i.e., least covalent) $Cs^+\cdots S^{2-}$ interactions. In turn, a more electron rich moiety can be more prone to lose an electron. In Figure 2, representations of the crystal structures of KMS-1 and its Rb^+- and Cs^+-exchanged analogues are provided along with the indication of the a axis, corresponding M−S bond distances and interlayer spacing values.

Because the ion-exchange reactions were conducted in air, the oxidation of Mn^{2+} to Mn^{3+} presumably occurs via electron transfer to atmospheric O_2. To confirm that O_2 was responsible for the oxidation of Mn, a Cs^+ ion-exchange experiment was performed under anaerobic conditions (in a N_2-filled glovebox). The Cs^+-exchanged product of this reaction displayed a much higher Cs/Mn ratio of 1.5:1 (found by EDS) and an a axis ∼3.68 Å (very close to that of the pristine material). This result indicates significant suppression of oxidation of Mn^{2+} under N_2 atmosphere. It is nearly impossible, however, to avoid partial oxidation of Mn, since complete exclusion of O_2 from water is extremely difficult. Prepared pristine, by solid state reaction, the $Cs_{2x}Mn_xSn_{3-x}S_6$ compound displays a Cs/Mn ratio ∼2:1 (found by EDS) and an a axis ∼3.68 Å consistent with Mn^{2+}. Therefore, atmospheric O_2 is the electron acceptor for the oxidation of Mn^{2+}, during ion-exchange where the degree of oxidation is greater with increasing Lewis basicity of the cation.

XPS Study of the Mn and Sn Oxidation State in Pristine and Ion-Exchanged Cs^+, Rb^+ [$Mn_xSn_{3-x}S_6$]. The oxidation state of Mn in the pristine, Cs^+-, and Rb^+-exchanged compounds was probed with XPS. The observed Mn2p peaks were usually very broad and in most cases, were fitted with two deconvoluted peaks. XPS data for these compounds are given in Table 2 and Figure 3. On the basis of these data and comparison with

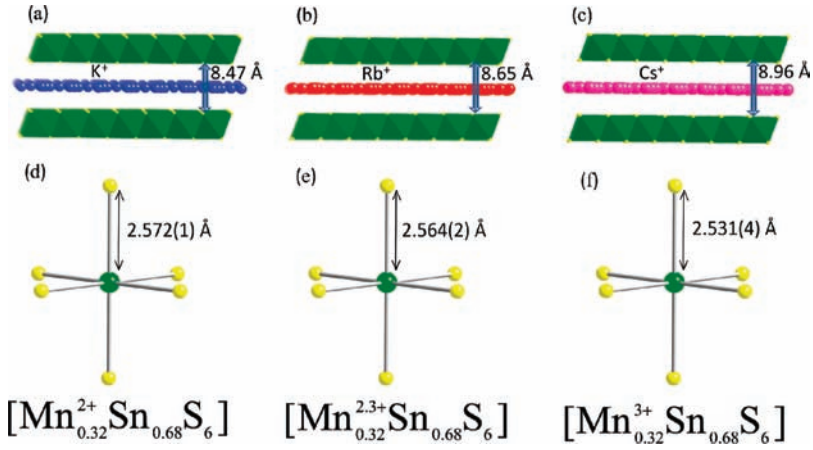

Figure 2. Representations of the crystal structures of KMS-1 (a), Rb-exchanged (b), and Cs-exchanged (c) materials viewed down the *b* axis. The (Mn, Sn)S_6 octahedra in the structures of KMS-1 (d), Rb-exchanged (e), and Cs-exchanged (f) materials, with the indications of M−S distances and the Mn oxidation state.

Table 2. XPS Data and Assignment of Sn, Mn Oxidation States for Pristine and Exchanged Materials

compound	type of synthesis	Mn2p (eV)	Mn^{2+}/Mn^{3+} ratio of integrals	$Sn3d_{5/2}$ (eV)	assignment
$K_{1.9}Mn_{0.95}Sn_{2.05}S_6$	solid state reaction	639.4, 640.4	–	486	Mn^{2+}, Sn^{4+}
$CsMn_{0.95}Sn_{2.05}S_6$	ion-exchange in air	640.6, 641.1	1/7.6	486.4	$Mn^{2.9+}$, Sn^{4+}
$Rb_{1.57}Mn_{0.95}Sn_{2.05}S_6$	ion-exchange in air	639.5, 640.8	–	486	$Mn^{2+\delta}$, Sn^{4+}
"$Cs_{1.5}MnSn_{2.2}S_6$"[a]	ion-exchange under N_2	640.3, 641.6	1/1.1	486	$Mn^{2.5}$, Sn^{4+}
"$Cs_2MnSn_{2.2}S_6$"[a]	solid-state reaction	639.2, 640.4	–	486.2	Mn^{2+}, Sn^{4+}

[a] Average formula obtained from EDS on polycrystalline samples.

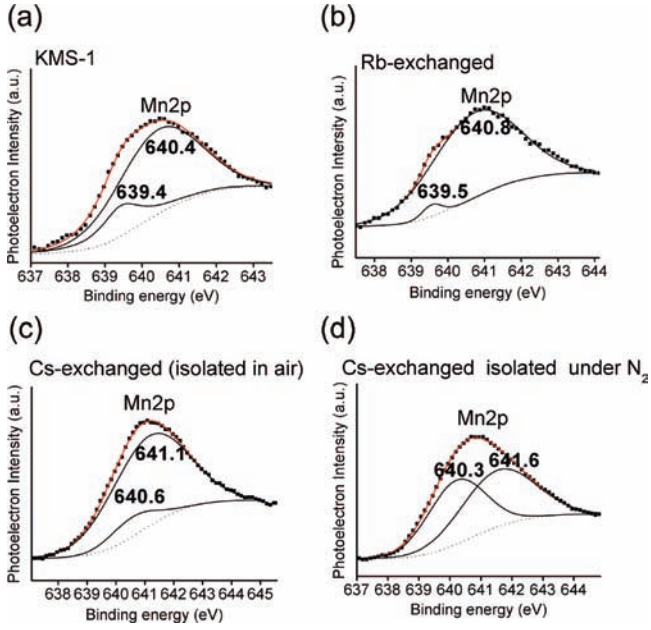

Figure 3. Mn2p peak in the XPS spectrum of (a) KMS-1, (b) Rb-exchanged, and (c) Cs-exchanged prepared in air and (d) Cs-exchanged prepared under N_2 atmosphere. The red and black solid lines represent the overall fitting and the deconvoluted peaks, respectively. The dotted lines represent the fitting of the background.

published data for the Mn2p binding energy in MnS,[45] we can assign a Mn^{2+} oxidation state for the pristine KMS-1.

The Mn2p binding energy for the Rb analogue is slightly higher (~ 0.4 eV) than that for the pristine material K analogue (and MnS), which is consistent with higher degree of oxidation. The Mn2p peak in the XPS spectrum of the Cs^+-exchanged material can be fitted as two peaks at 640.6 and 641.1 eV, Figure 3c. The peak at 641.1 eV may be attributed to Mn^{3+} ions.[45] Unfortunately, there is lack of XPS data for Mn^{3+} chalcogenide compounds. To our best knowledge, binary Mn sulfide or ternary Mn^{3+} sulfide phases have not been reported (although selenides and tellurides are known[46,47]). The ratio of the integrals of the two peaks at 641.1 and 640.6 eV may be assigned as the ratio of Mn^{3+} (641.1 eV) to Mn^{2+} (640.5 eV) which was calculated at ~7.6. This ratio indicates an oxidation state of Mn of ~3.

XPS data were also recorded for the Cs analogue produced by a solid state reaction, as well as for the Cs^+-exchanged compound prepared and isolated under N_2 atmosphere (Table 2, Figure 3d). The data are consistent with Mn^{2+} for the solid-state product and partial oxidation for the ion-exchanged material (estimated average Mn oxidation state ~2.5, see Table 2 and Figure 3d).

The $Sn3d_{5/2}$ XPS data are consistent with Sn^{4+} ions as expected (see Table 2 and Supporting Information).

Time Evolution of the Cs^+ Ion Exchange and Mn^{2+} Oxidation. Because of the concomitant Cs^+ exchange and oxidation of Mn^{2+}, we monitored this process as a function of time. Specifically, the products of exchange reactions performed for 2, 6, and 13 h were isolated and studied by XPS and PXRD. The XPS of the product at 2 h revealed a Mn2p binding energy of 641.1 eV (0.7 eV higher than that of the pristine material), which corresponds to a Mn^{3+} ion. PXRD data for the same product showed that the (003) peak shifted to lower 2θ values ($c = 27.14$ Å) and the (110) peak (indicating a shorter *a* axis at 3.64 Å) shifted to higher 2θ values compared to those in the pristine material. The Mn2p binding energies and the *a*- and *c*-cell parameters for the products at 6 and 12 h did not differ significantly from those of the 2 h product (see Supporting

(45) http://www.lasurface.com/database/liaisonxps.php.

(46) Kim, J.; Hughbanks, T. *J. Solid State Chem.* **1999**, *146*, 217–225.
(47) Kim, J.; Wang, C.; Hughbanks, T. *Inorg. Chem.* **1999**, *38*, 235–242.

Table 3. Selected Data for Cs^+ Ion-Exchange Experiments

initial concentration (ppb)	51100	1140	1117	1117	30	30
(Molar ratios)						
Na/Cs	–	–	655[a]	655[a]	2.0×10^4[b]	2.0×10^4[b]
Ca/Cs			21[a]	21[a]	2.7×10^3[b]	2.7×10^3[b]
Mg/Cs			45[a]	45[a]	1.2×10^3[b]	1.2×10^3[b]
V:*m*(mL/g)	1000	1000	100	47	204	100
pH	7	7	11	11	7	7
Final concentration(ppb)	3300	53	103	12	11.4	12.1
% Cs Removal	93.5	95.4	90.8	98.9	62.0	59.8
K_d^{Cs} (mL/g)	1.4×10^4	2.1×10^4	9.9×10^2	4.1×10^3	3.3×10^2	1.5×10^2

[a] Reactions with potable water samples containing ~7 ppm Ca, 125 ppm Na, 9 ppm Mg, 6 ppm K. [b] Reactions with potable water samples containing ~24 ppm Ca, 106 ppm Na, 7 ppm Mg, 5 ppm K.

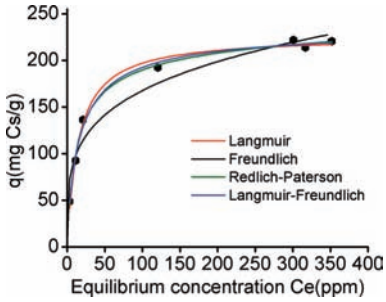

Figure 4. Equilibrium data for Cs^+ ion exchange (pH ≈ 7, $V/m = 1000$ mL/g, contact time ~12 h, initial Cs^+ concentrations in the range 55−550 ppm). The solid lines represent the fitting of the data with the various models.

Information). We can conclude from these results that the Cs^+ ion exchange and Mn oxidation are rapid and concurrent processes.

Cs^+ Remediation Properties of KMS-1. Sorbents selective for Cs^+ ions are particularly desirable, since they can be used for remediation of nuclear wastes and groundwater contaminated by ^{137}Cs.[39,40] Because of the promising ion-exchange results described above, we explored in more detail the Cs^+-remediation properties of KMS-1. Specifically, we performed Cs^+ ion-exchange equilibrium and kinetic studies and explored the effect of competitive cations and the acidity/basicity of the solutions on the Cs^+ absorption. Selected results are presented in Table 3. The ion-exchange equilibrium data are graphed in Figure 4. The fitting of the data with four different isotherm models, commonly used for the description of sorption and ion-exchange processes,[38,41,48−51] is given in Table 4. The models used were the

$$\text{a) Langmuir} \quad q = q_m \frac{bC_e}{1 + bC_e} \tag{1}$$

$$\text{b) Freundlich} \quad q = K_F C_e^{\frac{1}{n}} \tag{2}$$

$$\text{c) Langmuir−Freundlich} \quad q = q_m \frac{(bC_e)^{\frac{1}{n}}}{1 + (bC_e)^{\frac{1}{n}}} \tag{3}$$

$$\text{d) Redlich−Paterson} \quad q = \frac{AC_e}{1 + BC_e^g} \tag{4}$$

where q (mg/g) is the amount of the cation sorbed at the equilibrium concentration, C_e (ppm), q_m is the maximum sorption capacity of the sorbent, b (L/mg) is the Langmuir constant related to the free energy of the sorption, K_F and $1/n$ are the Freundlich constants and A, B, and g are the Redlich−Paterson parameters.[48]

The best fitting (correlation coefficient $R^2 \geq 0.99$) of the isotherm data was achieved with the Langmuir, Langmuir−Freundlich and Redlich−Paterson models (Table 4), while the fitting of the data with the Freundlich model was less satisfactory ($R^2 \approx 0.95$). The basic assumptions of the Langmuir model are that (a) the maximum sorption corresponds to a saturated monolayer of Cs^+, (b) all surface sites are equivalent and the energy of sorption is constant over all sites (i.e., the surface is homogeneous), and (c) the Cs^+ ions are sorbed at definite, localized sites and no transmigration of Cs^+ occurs.[48−51] In contrast, the Freundlich model assumes sorption on a heterogeneous surface, where the sorption sites exhibit a spectrum of different binding energies.[48−51] Langmuir−Freundlich and Redlich−Paterson are three-parameter models that reduce to the Freundlich and a linear isotherm at low surface coverage, respectively, while they are equivalent to Langmuir model for n or $g = 1$.[48−51] Looking at the structure of the Cs-exchanged material, it is apparent that all Cs^+ ions are arranged in a layer occupying the space between the metal sulfide layers (Figure 2c). In addition, the binding sites (i.e., S^{2-}) of the metal sulfide layers are, of course, equivalent and no transmigration of Cs^+ ions is possible after their incorporation into the interlayer space. Therefore, it seems that the Cs^+ exchange of KMS-1 is consistent with the assumptions of the Langmuir model and is thus reasonable to obey the Langmuir rather than the Freundlich model. Furthermore, the values of the constants n and g obtained with the Langmuir−Freundlich and Redlich−Paterson models respectively are close to 1, which also indicates the closeness of the model to the Langmuir isotherm.

The maximum Cs^+ exchange capacity q_m of KMS-1 was found to be 226(4) mg/g (or 1.70 mmol/g). As we described above, the Mn^{2+} of KMS-1 is oxidized to Mn^{3+} and thus, the observed Cs^+ exchange capacity (1.7 mmol/g) of KMS-1 is in good agreement with the maximum theoretical exchange capacity (~1.6 mmol/g) of $K_xMn^{III}_xSn_{3-x}S_6 \cdot 2H_2O$ ($x = 0.95$). This capacity compares well with that of the most efficient Cs sorbents (e.g., zeolites and zirconium−titanium silicates exhibiting capacities 1.86−4.1 mmol/g).[52−55] In addition, the distribu-

(48) Han, R.; Zou, W.; Wang, Y.; Zhu, L. *J. Environ. Radioact.* **2007**, *93*, 127–143.
(49) Calvet, R. *Environ. Health Persp.* **1989**, *83*, 145–77.
(50) Arias, M.; Perez-Novo, C.; Lopez, E.; Soto, B. *Geoderma* **2006**, *133*, 151–159.
(51) Do, D. D. In *Adsorption Analysis: Equilibria and Kinetics*; Imperial College Press: London, 1998; pp 13−17; 49−57.
(52) Moller, T.; Harjula, R.; Pillinger, M.; Dyer, A.; Newton, J.; Tusa, E.; Amin, S.; Webb, M.; Araya, A. *J. Mater. Chem.* **2001**, *11*, 1526–1532.
(53) Chang, H.-L.; Shih, W.-H. *Ind. Eng. Chem. Res.* **1998**, *37*, 71–78.
(54) Bortun, A. I.; Bortun, L. N.; Poojary, D. M.; Xiang, O.; Clearfield, A. *Chem. Mater.* **2000**, *12*, 294–305.

Table 4. Fitting of the Isotherm Data and the Cs^+ Sorption Constants Obtained with the Langmuir, Freundlich, Langmuir−Freundlich, and Redlich−Paterson Models

Langmuir			Freundlich			Langmuir−Freundlich				Redlich−Paterson			
q_e(mg/g)	b(L/mg)	R^2	K_F	n	R^2	q_e(mg/g)	b(L/mg)	n	R^2	A	B	g	R^2
226(4)	0.07(1)	0.992	54(10)	4.1(6)	0.948	236(11)	0.07(1)	1.2(2)	0.994	19(4)	0.12(5)	0.94(4)	0.995

tion coefficient K_d values for the Cs^+ exchange were found high in the range $3 \times 10^3-2 \times 10^4$ mL/g (Table 3) and they are well-comparable with the best Cs^+ sorbents.[56−58]

The value of the Langmuir constant b for the Cs^+ exchange was 0.07(1) L/mg or 9.3(1) L/mmol and is substantially smaller than the Langmuir constant b value [0.44(1) L/mg or 39(5) L/mmol) for the Sr^{2+} exchange of KMS-1.[38] This indicates the higher strength and affinity of absorption of the Sr^{2+} ions by KMS-1, as expected considering the bivalency of the strontium cations. Indeed, Sr^{2+}/Cs^+ competitive exchange data we reported indicate much higher K_d for Sr^{2+} vs Cs^+ exchange for V/m ratios ≥1000 mL/g (see Supporting Information, Table S2).[38] However, for lower V/m ratios (≤250 mL/g) KMS-1 shows similar distribution coefficient values for Sr^{2+} and Cs^+ (Table S2). The reasons for the increased Cs^+ removal capacity of KMS-1 at low V/m ratios are discussed below.

By reacting the Cs^+-exchanged material with large excess of KCl, complete exchange of the Cs^+ ions by K^+ ones can be achieved. The regenerated K^+-containing material showed ≥95% of the Cs^+ exchange capacity of the pristine KMS-1.

Cs^+ ion exchange experiments of KMS-1 with solutions of various pH (0.8−12) were also conducted. The results indicated that KMS-1 exhibits significant Cs^+ uptake in the entire pH range tested (Figure 5). Remarkably, KMS-1 displayed significant Cs^+ exchange capacities of ∼90 and 152 mg/g in pH values as low as 0.8 and 1.8, respectively. At pH ∼2.5, the Cs^+ exchange capacity of KMS-1 reaches ∼79% of the maximum theoretical one. The remarkable capture of Cs^+ by KMS-1 under strongly acidic conditions may be rationalized by the higher affinity of the soft sulfide-based layer of KMS-1 for the relatively "soft" Cs^+ ions over the hard proton ions. Layered manganese oxides such as Na−birnessite and Mg−buserite with structures similar with KMS-1 showed also good performance for removal of Cs^+ from acidic solutions (0.1 M HNO_3).[59] These materials, however, performed very poorly at alkaline conditions. The better performance of the layered manganese oxides under acidic condtions was attributed to a two-step exchange/phase transition process involving the initial formation of the H^+−birnessite and the subsequent exchange of H^+ by Cs^+ ions.[59] This may not be the case for KMS-1, since the performance of the material is similar in either acidic or basic conditions. The K^+ ions in KMS-1 are more mobile and, therefore, more easily exchangeable than those in birnessite-type compounds because of the wider interlayer space in the first material (8.5 Å for KMS-1 vs 7 Å for Na− or K−birnessite). In addition, the K−S interactions are weaker than the K−O ones, and therefore, K^+ ions are more loosely bond in sulfides.

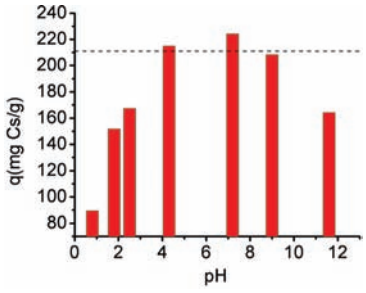

Figure 5. Variation of the Cs^+ exchange capacity of KMS-1 with pH. The dashed line represents the maximum theoretical exchange capacity calculated from the formula $K_xMn^{III}{}_xSn_{3-x}S_6 \cdot 2H_2O$ ($x = 0.95$).

The Cs^+ uptake values (mg Cs/g of KMS-1) at pH ≈ 4.3, 7, and 9 were found very close to the maximum theoretical value. A small drop of the Cs^+ uptake was observed at pH ∼12; however, KMS-1 showed a high Cs^+ exchange capacity of ∼164 mg/g (∼74% of the maximum theoretical one) even under these highly alkaline conditions.

The stability of Cs^+-exchanged KMS-1 over such a wide pH range is impressive. Both in acidic (pH ∼0.8−2.6) and alkaline environment (pH ∼12), the exchanged products retained the layered structure and high crystallinity (Figure 6) as well as high Cs^+ capturing ability. The excellent acid stability of Cs^+-exchanged KMS-1 is quite unusual for a sulfide compound, although recently it has been observed in metal selenides.[60−62]

To fully characterize the ion-exchange properties of KMS-1 we studied the kinetics of the Cs^+ exchange. Despite the relatively low Cs^+ concentrations (∼1 ppm) used for the kinetic experiments, the capture of Cs^+ by KMS-1 was rapid. Within only 5 min of solution/KMS-1 contact, the Cs^+ exchange reached its equilibrium with more than 90% of the initial Cs^+ amount removed from the solution (Figure 7). The extremely high mobility of the interlayer K^+ ions and the higher affinity

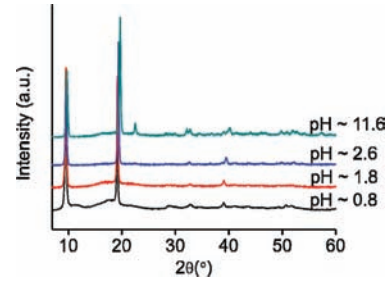

Figure 6. PXRD patterns of Cs-exchanged materials isolated at pH values of ∼0.8, 1.8, 2.6, and 11.6.

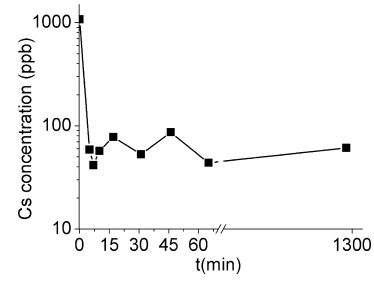

Figure 7. Kinetics of Cs^+ ion-exchange of KMS-1 plotted as the logarithmic values of the Cs^+ concentration (ppb) vs the time t (min). The small fluctuation of the data is not an error of the analysis, since it is reproducible. It may be due to the dynamic exchange process between K^+ and Cs^+, with the Cs^+ replaces K^+ ions immediately upon contact of KMS-1 with the solution and progressively a small fraction of K^+ ions re-enter the interlayer space of KMS-1 releasing some of the initial absorbed Cs^+ ions back to the solution.

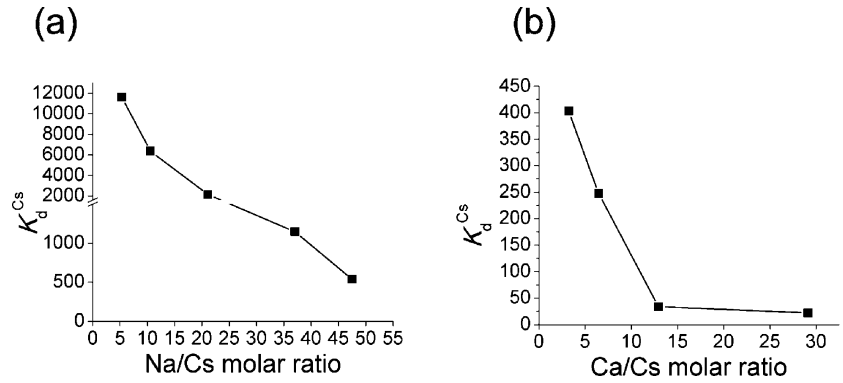

Figure 8. Variation of the distribution coefficient K_d^{Cs} with the (a) Na/Cs and (b) Ca/Cs molar ratios. The initial concentration of Cs^+ was ~52 ppm and the *V*/*m* ratio used was 1000 mL/g.

of the framework for the relatively "soft" Cs^+ ions over the harder K^+ ions can be considered the main reasons for the selective and very fast Cs^+ exchange.

Competitive Cs^+/Na^+ and Cs^+/Ca^{2+} experiments were also performed. Ca^{2+} was proven to be stronger competitor than Na^+ for the Cs^+ exchange of KMS-1. Specifically, high K_d^{Cs} values of $3 \times 10^3-10^4$ mL/g were obtained with the presence of 5−21-fold excess of sodium cations, while the K_d^{Cs} value was dropped below 10^3 mL/g for 50-fold excess of Na^+ ($K_d^{Cs} = 6 \times 10^2$ mL/g), Figure 8a. In contrast, the K_d^{Cs} values were found less than 10^2 mL/g with the presence of only 12-fold excess of Ca^{2+} (Figure 8b). It is reasonable to expect that the presence of a divalent cation such as Ca^{2+} in a relatively high excess would substantially affect the ion-exchange of a monovalent cation such as Cs^+.

Finally, we examined the Cs^+ exchange of KMS-1 under realistic conditions, with water solutions containing a variety of cations. Such water samples were created by adding ~1 ppm of Cs^+ to potable water and adjusting the pH of the final solution to ~11. The water samples thus prepared had close similarities (e.g., Ca^{2+}, Mg^{2+}, and Na^+ content and pH) with typical alkaline groundwater contaminated with radioactive elements. The results of the ion-exchange with such solutions (Table 3) indicated that KMS-1 was very efficient to absorb Cs^+, showing high removal capacities of 74−99% at *V*/*m* ratios of 50−500 mL/g, while much less Cs^+ removal (~38%) was observed at *V*/*m* ratio of 1000 mL/g. Actually, the data indicated an almost linear increase of the % Cs^+ removal by decreasing the *V*/*m* ratios (Figure 9).

The explanation for this behavior of KMS-1 is that at high *V*/*m* ratios the various competitive cations such as Ca^{2+}, Na^+ are present in excess (in relation to KMS-1) large enough to saturate almost all the exchange sites of KMS-1, thus limiting the Cs^+ exchange capacity of KMS-1. At lower *V*/*m* ratios, however, the amounts of the competitive cations were not longer sufficient for the complete saturation of the exchange sites of KMS-1, thus leaving more exchange sites available for Cs^+ ion exchange. Indeed, ICP-AES analytical data indicated significant K^+ content in exchanged samples (measured ratio K/Na/Mn = 1:1:2) obtained with $V/m \approx 500$ mL/g, while almost no K^+ was detected in samples obtained with $V/m \approx 1000$ mL/g.

We also tested the absorption capacity of KMS-1 with complex solutions containing very low Cs concentrations in the ppb range (~30 ppb). KMS-1 was efficient to absorb Cs under such conditions showing removal capacities ~60% for *V*/*m* ratios 100 and 200 mL/g (Table 3). Note that other competitive cations such as Ca^{2+}, Na^+, and Mg^{2+} were in molar concentrations $10^3-2 \times 10^4$ times higher than the initial Cs concentration; still, KMS-1 showed relatively good efficiency to absorb Cs.

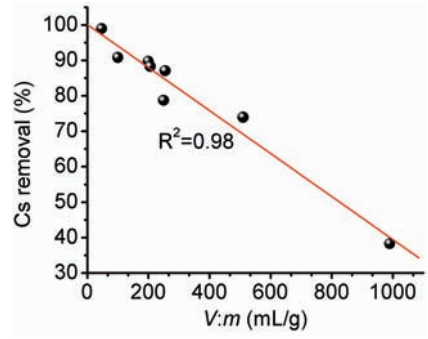

Figure 9. Percentage of Cs^+ uptake by KMS-1 from complex water solutions (pH~11, Ca ~ 7 ppm, Na~ 125 ppm, Mg ~ 9 ppm, K ~ 6 ppm, Cs ~ 1 ppm) versus the volume *V* (mL) of the solution to mass *m* (g) of KMS-1. The line represents the linear fitting of the data.

Concluding Remarks

The KMS-1 material showed facile and topotactic ion-exchange properties with Cs^+ and Rb^+ ions. The material exhibited high exchange capacity for Cs^+ retained under a very wide pH range (0.8−12). This is in marked contrast to the related layered manganese oxides being efficient only under acidic conditions and is attributed to the much higher mobility of K^+ ions in KMS-1 in relation to that of interlayer cations in the manganese oxides. The extremely high mobility of K^+ ions in KMS-1 is particularly reflected in the very fast kinetics of Cs^+ absorption by KMS-1 showing >90% removal capacity of relatively low Cs^+ concentrations within only 5 min of Cs^+/KMS-1 contact. KMS-1 was also effective to capture Cs^+ even in trace (ppb) concentrations from water samples with compositions similar to those of ground waters contaminated with radioactive ions. Therefore, KMS-1, which is an inexpensive material with a demonstrated reusability for Cs^+ exchange, may be considered as cost-effective sorbent for remediation of radioactive $^{137}Cs^+$ in such waters. It is also important that under

(55) Clearfield, A.; Bortun, A. I.; Bortun, L. N.; Poojary, D. M.; Khainakov, S. A. *J. Mol. Struct.* **1998**, *470*, 207–213.
(56) Bortun, A. I.; Bortun, L. N.; Clearfield, A. *Solvent Extr. Ion Exch.* **1997**, *15*, 909–929.
(57) Sylvester, P.; Clearfield, A. *Solvent Extr. Ion Exch.* **1998**, *16*, 1527–1539.
(58) Maslova, M. V.; Rusanova, D.; Naydenov, V.; Antzutkin, O. N.; Gerasimova, L. G. *Inorg. Chem.* **2008**, *47*, 11351–11360.
(59) Dyer, A.; Pillinger, M.; Harjula, R.; Amin, S. *J. Mater. Chem.* **2000**, *10*, 1867–1874.

certain conditions (i.e., with relatively low *V*/*m* ratios) KMS-1 shows similar selectivity for Sr^{2+} and Cs^+ and therefore it may be efficient for the removal of both $^{90}Sr^+$ and $^{137}Cs^+$ radionuclides from contaminated groundwater.

The exchange of KMS-1 with Cs^+ ions under atmospheric conditions is concurrent with an unusual topotactic oxidation of Mn^{2+} to Mn^{3+} in the layers. The exchanged compounds, thus obtained, constitute rare examples of stable Mn^{III}-containing sulfides. This oxidation and the consequent stabilization of Mn in the +3 oxidation state or even in mixed valence states, in combination with the ability of KMS-1 for intercalation of various metal and organic cations, makes KMS-1 an exciting new system for in depth magneto- and electrochemical investigations.

(60) Manos, M., J.; Malliakas, C., D.; Kanatzidis, M. G. *Chem.—Eur. J.* **2007**, *13*, 51–8.
(61) Ding, N.; Kanatzidis, M. G. *Angew. Chem., Int. Ed.* **2006**, *45*, 1397–1401.
(62) Manos, M. J.; Jang, J. I.; Ketterson, J. B.; Kanatzidis, M. G. *Chem. Commun.* **2008**, 972–974.

Acknowledgment. Financial support from the National Science Foundation (DMR-0801855) is gratefully acknowledged. Part of this work made use of the facilities in the Integrated Molecular Structure Education and Research Center (IMSERC) at the Northwestern University. A description of the facility and full funding disclosure can be found at http://pyrite.chem.northwestern.edu/analyticalserviceslab/asl.htm. This material is based upon work supported by IEC.

Supporting Information Available: CIF for the structures of K^+-, Cs^+-, and Rb^+-exchanged materials, TGA graphs for the Cs^+- and Rb^+-exchanged products, $Sn3d_{5/2}$ XPS spectra, Mn2p XPS spectrum for the Cs-analogue of KMS-1 synthesized with a solid-state reaction, XPS-PXRD graphs for the variable-time Cs^+ exchange experiments and Sr^{2+}/Cs^+ competitive ion-exchange data. This material is available free of charge via the Internet at http://pubs.acs.org.

JA900977P